**ACTA IMEKO**
**ISSN: 2221-870X**
*March 2026, Volume 15, Number 1, 1 – 9*

# Measurement of the frontal area of a swimmer: Alternative methods and uncertainty analysis

**Paolo Castellini[1], Alberto Scocco[1], Alessia Caputo[1]**

[1] *Department of Industrial Engineering and Mathematical Sciences, Polytechnic University of Marche, Ancona, Italy*

ABSTRACT
This study presents and validates two simplified methods to estimate the frontal area of swimmers during active motion, based on video recordings from frontal and lateral views. The aim is to provide low-complexity and practical tools suitable for use in some everyday sport training environments, such as swimming pools. The frontal view enables a direct measurement of the true projected area, but is affected by factors such as the water transparency and the variable swimmer-camera distance. Although providing only a 2D projection, the lateral view benefits from a short working distance and good stability, improving the analysis of posture-related features such as body alignment and angle of incidence.
By tracking and analyzing the evolution of the frontal area over the stroke cycle, the proposed methods allow the separation of propulsive and resistive contributions, revealing stroke-specific technical patterns. The results show that this approach can detect changes in technique, posture, and performance across different swimming styles and for the same athlete under varying conditions. Despite limitations in absolute accuracy due to simplified calibration and environmental variability, the system demonstrates sufficient repeatability and sensitivity for comparative analysis. The methods support biomechanical evaluation and feedback, contributing to technique refinement and improved swimmer performance.

**Section:** RESEARCH PAPER

**Keywords:** swimmer frontal area; posture analysis; propulsion and resistance; AI model; computer vision; sports biomechanics

**Citation:** P. Castellini, A. Scocco, A. Caputo, Measurement of the frontal area of a swimmer: Alternative methods and uncertainty analysis, Acta IMEKO, vol. 15 (2026) no. 1, pp. 1–9. DOI: 10.21014/actaimeko.v15i1.2230

**Section Editor:** Francesco Lamonaca, University of Calabria, Italy

**Received:** October 14, 2025; **In Final Form:** February 16, 2026; **Published:** March, 2026.



**Funding:** No funding specified.

**Corresponding Author:** Paolo Castellini, e-mail: p.castellini@staff.univpm.it

## 1. INTRODUCTION

The study of swimming hydrodynamics involves significant challenges due to the complexity of fluid-body interactions, the variability of human movements, and the practical difficulties of acquiring accurate data in water. In swimming practice, from a biomechanical perspective, the reduction in time to cover a certain distance depends on two factors. The first is the improvement of propulsion, which is produced mainly through coordinated movements of the arms and legs. The second is to minimize the resistive force of hydrodynamic drag, which opposes motion in water.

The hydrodynamic drag is influenced by the posture, body shape, frontal area, and movement patterns of the swimmer. In recent years, increasing attention has been paid to techniques aimed at quantifying these contributions under real swimming conditions, with particular focus on Projected Frontal Area (PFA) and body alignment.

Numerous studies have explored these aspects using different methods and technologies. For example, Cortesi et al. analyzed the variability of arm-stroke temporal descriptors within and between laps using Inertial Sensors (IMUs) [1]. They combined IMU orientation data with a biomechanical model of the upper limb to estimate the 3D trajectory of the wrist in real time. Similarly, Crenna et al. performed in-pool experiments using IMU-based systems, supported by laboratory validation with an optoelectronic motion capture system [2].

Passive drag has been estimated using electromechanical towing systems, as in Cortesi et al. [3], where standing and streamlined positions of the swimmer were measured. Although useful, these measurements did not directly address the frontal area. Active drag, on the other hand, has been evaluated using both full and semi-tethered swimming protocols, allowing the inference of resistive forces under near-natural swimming conditions [4]. A related approach is presented in Gatta et al., where tethered swimming tests were used: assessing drag at maximal effort and estimating hand velocity via 3D kinematics or a paddle-wheel model, they related propulsive force to hydrodynamic resistance [5].

Some studies opted for more indirect approaches. In Kolmogorov et al., for example, drag was estimated by comparing swimming performances with and without added resistance, under the assumption of constant power output [6]. This approach highlighted how individual differences in swimming technique significantly affect the drag coefficient. Similarly, Toussaint et al. (2004) compared two drag estimation methods: the Measuring Active Drag (MAD) system and the Velocity Perturbation Method (VPM). This study revealed how each method captures different aspects of hydrodynamic resistance [7].

Over the last three decades, research on swimming hydrodynamics has progressively evolved from indirect drag estimation methods and simplified models, mainly developed in the 1990s and early 2000s [6], [7], toward in-pool experimental approaches and image-based analyses. In particular, from the mid-2010s onward, increasing attention has been paid to techniques capable of capturing stroke-resolved kinematics, posture, and frontal area variations under real swimming conditions, supported by advances in computer vision and artificial intelligence.

Other authors have focused on PFA estimation with image-based analysis. Naemi et al. measured glide performance by analyzing swimmers in a horizontal position, approximating their cross-sectional area using ellipses [8]. In Gatta et al., the planimetric method was applied using underwater cameras to estimate the frontal area throughout the stroke cycle [9]. However, these methods required manual frame-by-frame analysis and were heavily dependent on the swimmer's position relative to the camera, limiting both reproducibility and scalability.

To overcome these limitations, video-based markerless systems have been proposed. Ceseracciu et al. developed a system that estimates joint positions and velocities during freestyle swimming by automatically extracting 3D coordinates from video frames, validated against traditional manual digitization [10]. More recently, deep learning techniques have enabled the robust and automated extraction of swimmer posture. For example, Giulietti et al. employed neural networks such as OpenPose and YOLO to detect body landmarks and evaluate the trajectories of body key points [11], [12], [13].

Recent reviews have highlighted the rapid expansion of video-based and markerless motion analysis in biomechanics, driven by advances in deep learning and camera-based pose estimation, with increasing applicability in real-world and in-field conditions [14].

In the specific context of swimming, recent surveys have emphasized the growing role of artificial intelligence and computer vision techniques for performance analysis, posture assessment, and kinematic feature extraction from video data [15].

Furthermore, vision-based approaches have been proposed to estimate frontal area and to relate kinematic features to hydrodynamic quantities such as instantaneous active drag under realistic swimming conditions [16].

These developments further support the use of camera-based and AI-assisted methods for stroke-resolved and posture-aware swimmer analysis, as adopted in the present study.

In parallel with these developments, recent studies (2021–2025) have emphasized the importance of longitudinal and intra-subject analysis for technique assessment and performance progression in swimming [17]. Furthermore, recent advances in biomechanical modeling (2024–2025) have enabled a more refined interpretation of PFA variations across stroke phases and body segments [18], [19], while comprehensive biomechanical analyses have clarified the respective roles of propulsion and resistance in different swimming styles.

Building on these recent advances, Washino et al. presented further refinements in geometric modeling, where the PFA of each body segment was calculated by combining reflective marker data with 3D scans of the swimmer's body [18]. Their results showed that the contribution of the upper limb segments to pressure drag tends to be overestimated when analyzed under static conditions. In a follow-up study, Washino et al. examined the relationship between swimming velocity and vertical displacement of the center of mass (CoM) in different stroke phases. This showed phase-specific dependencies between technique and drag-related body positions [19].

Finally, Morais et al. studied the influence of frontal surface area and stroke velocity variations during the front crawl, comparing land-based and in-water Frontal Section Area (FSA) measurements at key moments of the arm pull [20]. These values were correlated with power estimates obtained through the VPM. This reinforces the relevance of the frontal area for evaluating the swimmer's movements.

These approaches have significantly advanced our understanding of swimming hydrodynamics and highlighted the necessity of a trade-off: accurate methods often require complex equipment and setups, limiting their applicability in everyday coaching scenarios. In contrast, simpler methods may lack precision and repeatability.

This study aims to address this gap by comparing two video-based methods-frontal and lateral camera perspectives-to estimate the swimmer's PFA throughout the stroke cycle. The focus is on an approach that is simultaneously non-invasive, coach-friendly, and metrologically robust. Special attention is paid to assess the uncertainty of the measurement and to distinguish the propulsive and resistive phases of the stroke. The analysis is centered on the athlete: anthropometric differences (including gender) are not directly addressed, as the main goal is to support the individual optimization of technique, trim, and posture, rather than making comparisons between groups of swimmers.

## 2. MATERIALS AND METHODS

The performance of swimming depends on several interrelated factors, among which muscle power, the efficiency of propulsive motion, and the ability to minimize drag play a central role. From a hydrodynamic point of view, the total resistance acting on a swimmer depends, through the properties of the fluid, on the sum of three main components [21]:

- *Wave drag*, generated by the motion of the swimmer at the free surface and very significant in swimming;
- *Skin friction*, caused by the viscosity of water acting on the swimmer's skin;
- *Pressure drag*, due to the pressure difference between the front and rear of the swimmer.

Wave drag represents a major contribution to total resistance, but it is also very difficult to evaluate and optimize, especially in the case of a swimmer whose shape continuously changes due to limb and body movements.

Skin friction depends essentially on the 'wet surface' of the body; considering that current competition regulations do not allow the use of full-body swimsuits, improvements in swimming performance through the reduction of skin friction are limited.

Pressure drag depends on the shape and size of the body, making it possible for swimmers to work on hydrodynamic positioning to improve gliding. Pressure drag is almost the only drag contribution

Figure 1. Schematic representation of the swimmer's PFA and ULS.

that can be optimized in swimmers' training, and is the focus of this work.

As schematically represented in Figure 1, the pressure drag can be modeled under the assumption of motion in a fully submerged condition. In this context, the resistive force $R$ acting on the swimmer is described by the well-known equation:

$$R = A \cdot C_D \cdot \frac{1}{2} \rho v^2, \quad (1)$$

where:
- $\rho$ is the density of water;
- $v$ is the swimmer's velocity relative to the fluid;
- $C_D$ is the drag coefficient;
- $A$ is the PFA in the direction of motion.

In this formula, the frontal area of the swimmer is a key determinant of drag and represents an important parameter to evaluate hydrodynamic efficiency throughout the stroke cycle, not only during the passive glide phase.

On the other hand, from a swimmer hydrodynamic perspective, frontal area can be subdivided into two main components:
- the **PFA**, which corresponds to the passive portion of the body and contributes directly to drag;
- the **ULS** (Upper Limb Stroke), primarily involved in propulsion and thus associated with a negative drag effect.

The dynamic evolution of the frontal area during the swimming cycle reflects the resistance and propulsion phases. Valuable insight into swimmer posture and technical execution comes from the separation of passive and active contributions.

The objective of this work is to develop a practical, low-cost system to estimate the frontal area swimming in standard training environments. The aim is to avoid complex and expensive setups involving multi-camera systems, elaborate calibration procedures, or external synchronization hardware.

### 2.1. Experimental setup

Data are acquired with a single underwater action camera (GoPro-type), placed at a depth of approximately 30 cm. Two different acquisition perspectives were considered:
- **Frontal view**: captures the swimmer approaching the camera;
- **Lateral view**: observes the swimmer from the side over a portion of the stroke.

The two acquisition configurations present complementary advantages and limitations in terms of measurement robustness, uncertainty sources, and applicability in training environments. A structured comparison of the two approaches is provided in Table 1.

The video frames are processed using two deep learning solutions: the You Only Look Once (YOLO) model from Ultralytics and the Segment Anything Model v2 (SAM 2) developed by Meta, as shown in Figure 2.

YOLO is an AI suite that provides a wide variety of tools, from object detection to body pose assessment, and allows trained and untrained working modalities, such as SAM 2. It is used only to process the images that initially come from the camera, to locate the Region of Interest (RoI) centered on the swimmer's body, and then crop it. This improves the effectiveness and efficiency of the subsequent elaboration from SAM 2 .

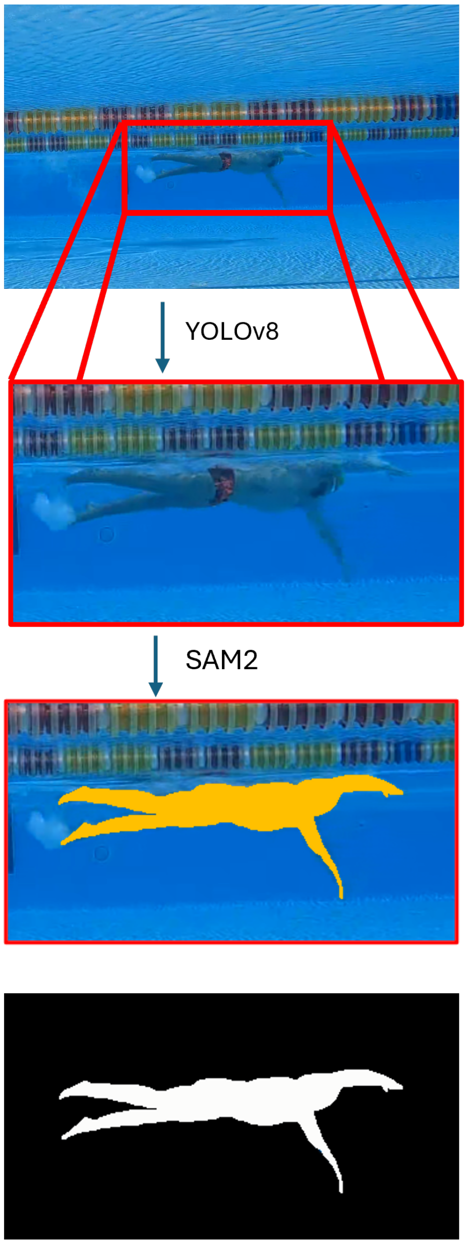


Figure 2. Pipeline for lateral view video-processing.

The pretrained YOLOv8x and SAM 2.1 Hiera Large models were selected for object detection and segmentation, respectively. Given that real-time latency is not a constraint, these models deliver high-quality results off-the-shelf, eliminating the need for task-specific training.

SAM 2 performs automatic segmentation of objects in each frame with 'temporal data handling': it allows users to set points of interest in a frame, produce the segmented areas in the frame, and then follow the evolution of the segmented area in the subsequent frames. SAM 2 also includes untrained 'zero-shot' segmentation functions to produce masks even for unseen images: it made quite good predictions over the areas of interest of the swimmer, without the need of a specific training or to add refinement points.

SAM 2 enables segmentation by specifying positive (foreground) and negative (background) points on the first frame of a video sequence.

Table 1. Summary comparison between frontal and lateral video acquisition methods.

<table>
<tr><th></th><th>Frontal view</th><th>Lateral view</th></tr>
<tr><td rowspan="2">Advantages and suitable use cases</td><td colspan="2">Sufficient repeatability for comparative analyses<br>Consistency analysis of repetitive stroke cycles<br>Sufficient reliability to detect variations and to differentiate technical elements or posture differences<br>Consistent comparisons within the same swimmer between sessions or experimental conditions<br>Suitable for tracking intra-athlete changes or evaluating technical interventions by swimming coaches</td></tr>
<tr><td>- Easier recording setup, due to single swimmer session acquisition<br>- Emphasizes overall body alignment and symmetry<br>- Allows a more direct measurement of the projected area, closely corresponding to the true frontal section</td><td>- Clearer separation of resistive and propulsive contributions<br>- Some movement effects are clear and prominent<br>- Reduced operational distance and more stable optical conditions<br>- Enhances the visibility of body posture and body orientation, including pitch and roll angles</td></tr>
<tr><td rowspan="2">Limitations and uncertainty sources</td><td colspan="2">Absolute accuracy is limited by the simplified setup<br>Bubbles, foam or surface reflections impacting segmentation accuracy<br>Water turbidity and movement, and light scattering, particularly at longer distances and in proximity to the swimmer</td></tr>
<tr><td>- Variation in scale due to changes in swimmer–camera distance<br>- Camera resolution, which influences pixel-based area estimation</td><td>- Calibration based on athlete's body height, subject to anthropometric variability<br>- Lens distortion and refraction effects due to underwater acquisition<br>- Floating lane divider movements<br>- Variable silhouette resolution depending on the swimmer's distance from the camera<br>- Occlusions or interference from multiple swimmers</td></tr>
</table>

Independently of the frame rate and image resolution, SAM 2:
- performs the initial segmentation based on the user-defined points;
- propagates and adapts the segmentation mask to subsequent frames using a memory-bank approach;
- allows refinement through the addition of further positive or negative points to correct tracking errors from a given frame onward.

The AI models were deployed on a dedicated workstation with the following hardware and software configurations:
- CPU: Intel Core i7-11700 with 64 GB RAM;
- GPU: two Nvidia RTX 3090 boards with 24 GB VRAM each;
- Operating system: Linux Ubuntu 22.04 LTS (64-bit), with Nvidia driver version 550.163.01.

These video processing modalities and specific strategies for frontal and lateral acquisition aimed to fully automate the analysis, improve robustness, and eliminate operator biases.

### 2.1.1. Frontal view

The frontal acquisition captures the swimmer approaching the camera, from a distance of between 25 meters and 2 meters. These perspective and scaling variations introduce significant challenges: as the swimmer gets closer, the image of the body progressively enlarges, leading to strong variations in pixel-based area measurements. To address this configuration, the video frames were processed in reverse temporal order, starting with frames where the swimmer is closest to the camera. This helps in the initialization of SAM 2, as the swimmer appears large and centered in the frame. SAM 2 then propagates the segmentation backwards, across subsequent frames as the swimmer seems to recede. The frontal area in each frame is evaluated as the number of pixels within the segmented mask, and represents a 2D projection of the swimmer's body. Taking into account the variation of the distance from the camera, these raw values require correction, as shown in Figure 3.

This relationship derives from the perspective projection geometry. According to the pinhole camera model (shown in Figure 4),

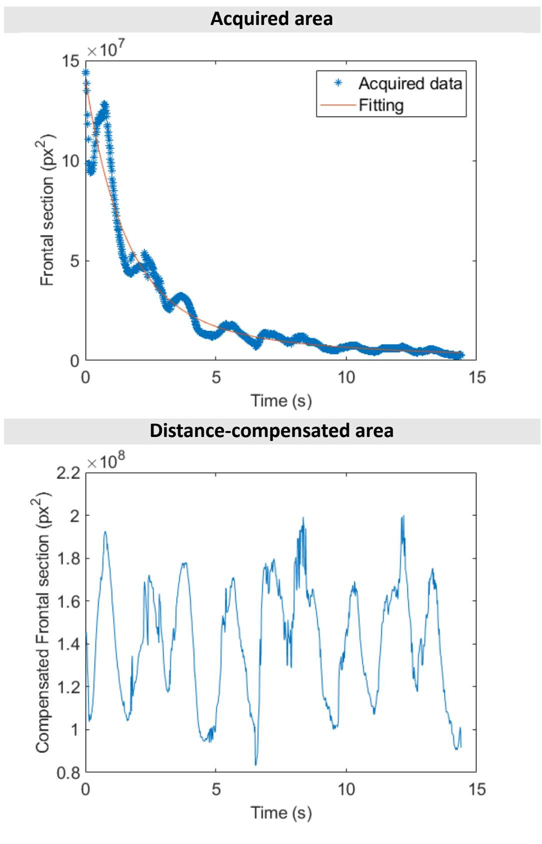


Figure 3. Perspective correction in frontal acquisition. Left: raw area values. Right: compensated values assuming constant speed.

the relationship between image size, object size, focal length, and working distance can be expressed as:

$$\frac{Image}{Object} = \frac{f}{d}, \tag{2}$$

where $f$ is the focal length of the lens and $d$ is the swimmer–camera distance. Assuming a fixed focal length and uniform swimmer motion, the swimmer–camera distance can be expressed as $d = v \cdot t$, where $v$ is the swimmer speed. Under these conditions, the image magnification is inversely proportional to the distance:

$$M = \frac{Image}{Object} \propto \frac{1}{d} = \frac{1}{v \cdot t}, \tag{3}$$

and, consequently, the apparent projected area follows an inverse square relationship:

$$A \propto \frac{1}{d^2}. \tag{4}$$

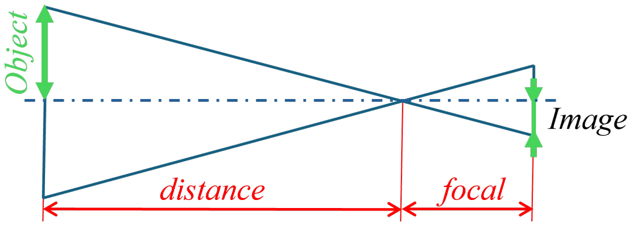


Figure 4. Schematic representation of the pinhole camera model.

Fitting the raw area profile with the theoretical curve, a correction can be applied to compensate for perspective distortion. This yields area estimates consistent with a constant distance, enabling inter-trial comparisons and conversion to physical units (e.g., square meters) with additional calibration.

### 2.1.2. Lateral view

In the lateral configuration, the camera observes the swimmer from a side field about 6 meters long: it covers approximately 2 or 3 stroke cycles. To ensure the entire framing of the swimmer's body in the path, the camera is placed at a distance of roughly 6 meters. This approach does not aim to provide a metrically accurate estimate of the swimmer's frontal area, but rather an indirect proxy derived from a 2D side projection. It is therefore primarily suited for intra-subject comparisons (e.g., technique and posture variations) and for relative analyses under the same acquisition setup. Its use as an absolute measure of frontal area in physical units would require a dedicated 3D model and calibration.

Lateral images are affected by water turbidity and motion blur, particularly in the limbs. To improve robustness, each frame is first processed using the YOLO tool for object detection, to settle a Region of Interest (RoI) centered on the swimmer's body, and then crop it. This:

- reduces data size, to improve the processing efficiency;
- ensures that the swimmer is centered, to facilitate the subsequent SAM 2 initialization.

Then SAM 2 is used to segment the swimmer's profile in each frame. A vertical projection of the mask produces a simplified frontal profile of the swimmer, from which the maximum vertical extension is extracted as a proxy for the frontal area, as shown in Figure 5.

This method assumes a two-dimensional swimmer model that has uniform thickness across body segments and overestimates the contribution of the limbs relative to the torso. Although not dimensionally accurate, this approach is valuable for analyzing intra-cycle and inter-cycle variations, as well as for comparing different athletes under the same conditions.

To simplify the calibration procedure, the swimmer's actual height was used to scale the pixel measurements, avoiding the need to set physical targets or synchronized instrumentation.

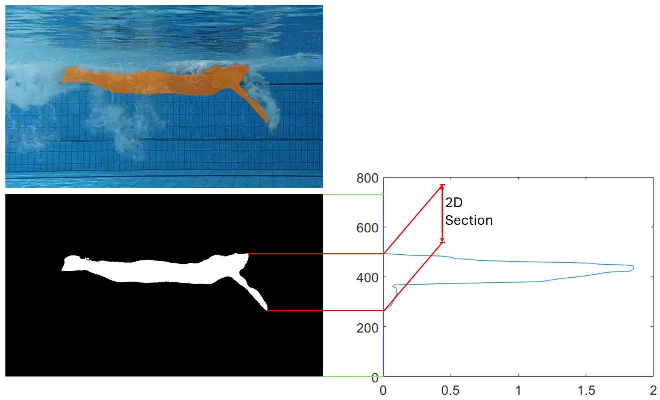


Figure 5. Left: lateral segmentation mask at t=0. Right: vertical projection profile in the subsequent 2 seconds.

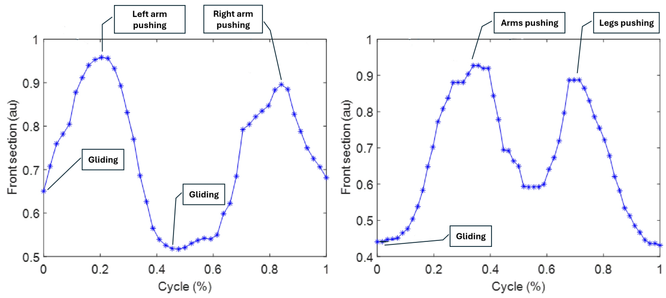


Figure 6. Temporal evolution of the frontal area during a stroke cycle: comparison of freestyle on the left and breaststroke on the right.

## 3. RESULTS

This section presents the results obtained with video acquisitions from the frontal and lateral perspectives and highlights the evolution of the frontal area of the swimmer throughout the stroke cycle. The two perspectives are complementary: the frontal view emphasizes overall body alignment and symmetry, while the lateral view offers a clearer separation of resistive and propulsive contributions.

### 3.1. Frontal view results

Figure 6 shows the variation of the PFA throughout a complete stroke cycle, comparing freestyle and breaststroke. Frontal area values are expressed in arbitrary units (a.u.), as the signals are normalized to emphasize relative temporal variations rather than absolute calibration. In freestyle, the alternating thrusts of the right and left arms produce a near sinusoidal pattern, although not perfectly symmetric for the swimmer analyzed. Glide phases are present but exhibit asymmetry, reflecting individual technical execution.

The breaststroke pattern is markedly different, with a clear symmetry between arm and leg thrusts. The cyclical alternation between propulsion and glide is more regular, with well-defined phases corresponding to arm pull, leg kick, and recovery.

Figure 7 illustrates six key moments within the breaststroke cycle, marked with a red dot on the curves of the frontal area. These images demonstrate how the frontal area varies significantly in function of body pose during the stroke (note that the images suffer scale variations due to distance from the camera, while the curves are compensated, as previously described).

The analysis of the frontal area reveals that significant variations occur during each stroke, with maximum values reached during the propulsive arm phase and minimum values during glide. However, not all increases in the frontal area can be attributed

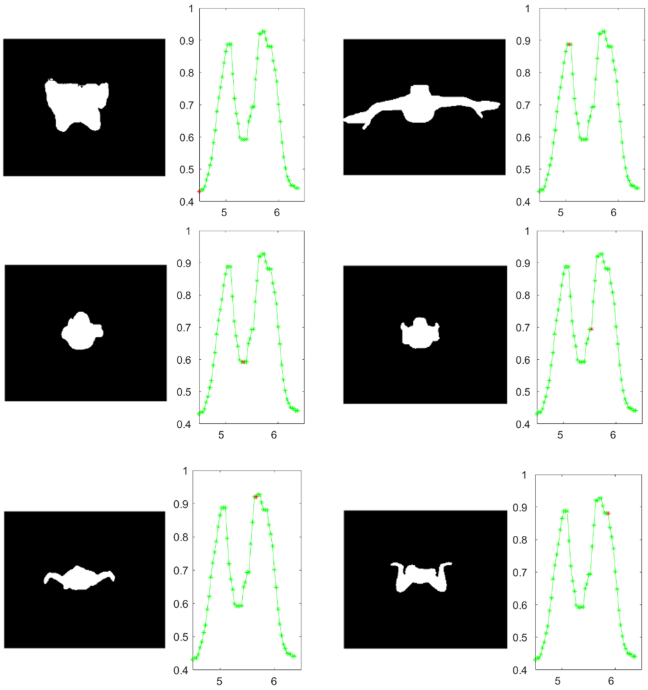

Figure 7. Key phases of the breaststroke cycle and their frontal area values, with distance factor correction. Each image captures a specific instant during the stroke (marked by the red dot on the frontal area curve) and shows how changes in body shape configuration affect the projected frontal area.

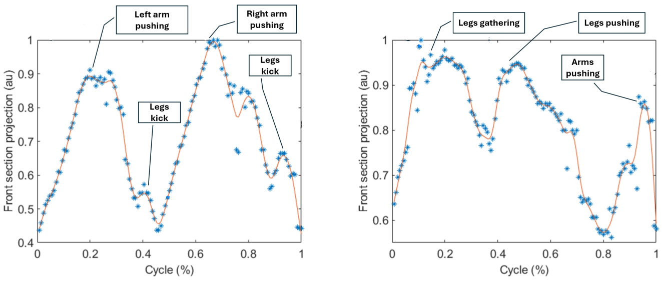


Figure 8. Frontal area variation from the lateral view: comparison of freestyle and breaststroke.

to increased drag: for example, during arm extension, the arms contribute positively to propulsion rather than resistance [22].

Although the body's frontal area is generally associated with resistive drag, the contribution of the arms is primarily propulsive and thus beneficial to performance. Similarly, the role of the legs varies with stroke style, but is generally minor in terms of resistive contribution, though not negligible.

Separating resistive and propulsive contributions from the frontal area over time allows a clearer understanding of the swimmer's technique and its biomechanical efficiency.

### 3.2. Lateral view results

Figure 8 presents the frontal area estimated from the lateral perspective. The temporal evolution highlights the different phases of the stroke cycles in the freestyle and breaststroke. In freestyle, the characteristic double periodicity—two strokes and two kicks per cycle—is evident. In contrast, breaststroke shows a symmetric pattern with synchronous movement of the limb.

In breaststroke, the most pronounced variations are due to leg recovery and propulsion. The recovery phase increases the frontal area and introduces resistive drag, while the kick produces thrust [23]. This distinction between the resistance and propulsion phases is effectively captured in the lateral projection.

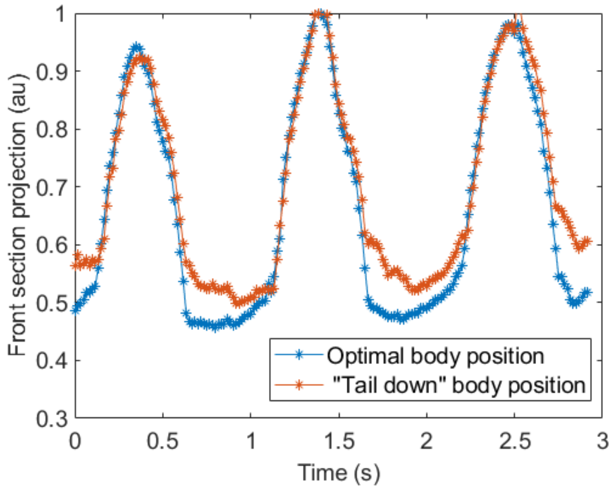


Figure 9. Comparison of frontal area in two different buoyancy configurations: horizontal alignment vs. tail-down posture.

Compared to frontal-view analysis, some effects, such as leg kicks in freestyle or arm thrusts in breaststroke, are more prominent. This is due to the overestimation caused by the horizontal projection: body parts such as feet or hands appear larger when viewed laterally, even if they are small.

These situations lead to some overestimation in absolute values and demonstrate the usefulness of identifying stylistic differences when swimmers or techniques vary.

The minima in the curves of the frontal area correspond to the glide phases. The duration of these low-resistance intervals varies with the swimmer's technique and thrust duration. The value of the minimum itself reflects the morphology and posture of the body. In particular, it shows the swimmer's ability to maintain a streamlined and horizontal alignment.

Figure 9 shows a comparison of two runs by the same athlete, with two different postural configurations. In the first run, the swimmer adopted a horizontal body position, optimized for minimal drag. In the second run, a 'tail-down' position was simulated by reducing leg buoyancy.

The upper region of the curves is related to the thrust of the arm and is almost identical. In the lower section, there is a substantial increase in frontal area due to altered posture. This confirms that the technique and position of the lower limbs significantly affect overall resistance.

To further separate resistive and propulsive contributions, it was possible to distinguish two different parts of the lateral area:

- the one due to the torso, which can be considered passive;
- the one due to the arms, which is active and gives thrust.

SAM 2 generates masks for the entire body, but it is possible to manually refine its results, evaluating the different areas, to obtain the profiles for the complete body and the torso only as in (Figure 10).

These results enable a detailed assessment of the athlete's technical performance. High peaks in the propulsive portion of the curve indicate strong thrust, while larger plateau-shaped profiles suggest sustained force application, typically associated with more effective and efficient techniques.

To synthetically compare different strokes or swimmers, we introduce a performance index based on the net impulse: the area under the thrust curve minus the area under the resistance curve. It is possible to consider this value to be proportional to the net change in momentum imparted by the stroke.

Figure 11 shows this metric computed over three consecutive strokes, highlighting intrasubject variability.

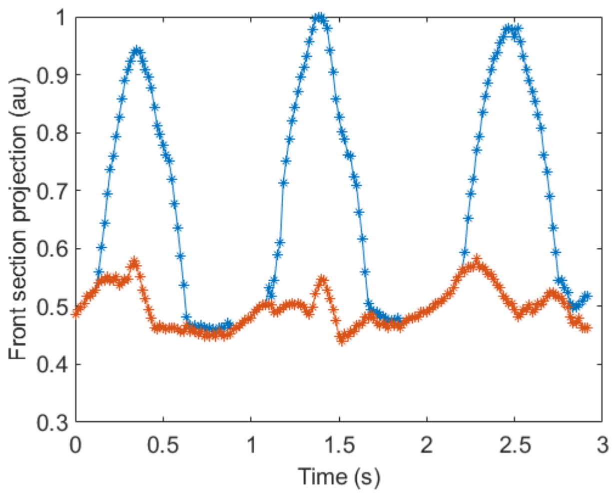


Figure 10. Comparison of frontal area curves: complete body (blue line) vs. torso only (red line).

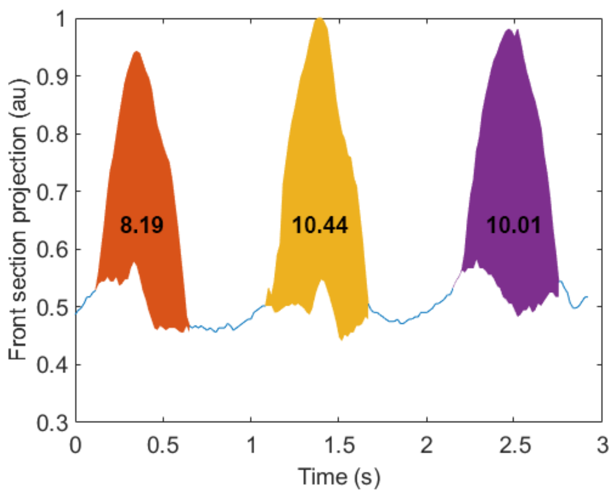


Figure 11. Net impulse (thrust area minus resistance area) across three consecutive strokes.

## 4. UNCERTAINTY ANALYSIS

The system presented in this study proposes two practical solutions for estimating the frontal area of a swimmer during motion. Both approaches were designed with minimal instrumentation and setup, making them suitable for routine use in training environments. To enable this, several simplifications were made in the measurement and calibration procedures.

This facilitates implementation and introduces trade-offs, particularly in terms of absolute accuracy. The system is not intended for the high-precision measurement of the frontal area, but rather to evaluate relative changes, to enable comparisons between swimmers or different configurations adopted by the same swimmer (e.g., posture adjustments suggested by a coach).

In this context, instrumental uncertainty is less critical than the intrinsic variability of the human body and its motion. Indeed, the key challenge lies in the reproducibility of the movement, rather than in the repeatability of the measurement system itself.

Parameters such as camera resolution or the perimeter-to-area ratio of the segmentation mask influence the measurement quality, but their impact is modest compared to the dynamic variability of swimming technique, limb motion, and water interaction. However, identifying and controlling key sources of uncertainty remains essential to ensure meaningful and consistent data.

We summarize the main sources of uncertainty for the two acquisition modalities:

*Frontal view:*
- Variation in scale due to the change in the swimmer–camera distance;
- Water turbidity and light scattering, particularly at longer distances;
- Presence of bubbles and foam affecting the segmentation accuracy;
- Camera resolution, which influences pixel-based area estimation.

*Lateral view:*
- Calibration based on the athlete's body height, subject to anthropometric variability;
- Water movement and turbulence in proximity to the swimmer;
- Lens distortion and refraction effects due to underwater acquisition;
- Bubbles or surface reflections impacting mask quality;
- Floating lane dividers movements;
- Variable silhouette resolution depending on the swimmer distance from the camera.

Additional complications can arise from these two factors:
- the non-static background of underwater environments, where turbulence and residual wake motion occur;
- the non linear effects of camera algorithms to contrast the lens distortion, when the swimmer's movement covers wide sections of the scene.

These factors can introduce variability that can also affect segmentation.

Despite these limitations, the system:
- shows sufficient reliability to detect variations and to differentiate technical elements or posture differences;
- allows for consistent comparisons between the same swimmer in sessions or experimental conditions.

### 4.1. Residual analysis

To evaluate the quality of the adjustment procedure applied to the frontal area data, the residuals between the measured values and the fitted model were analyzed over a normalized cycle. Figure 12 presents the curve of the frontal area (top) along with the corresponding percentage residuals (bottom).

The residuals remain within $\pm 2\%$ almost throughout the entire cycle, with local peaks up to $\pm 5\%$ for specific intervals. These larger deviations typically occur during phases of rapid limb movement or posture transitions, where segmentation can be affected by motion blur, bubbles, or light scattering. The overall distribution of residuals supports the suitability of the fitted model for cycle normalization and inter-trial comparisons, despite its limited ability to capture abrupt morphological variations.

## 5. CONCLUSIONS

The study introduced and validated two simplified methods for estimating the frontal area of a swimmer during active motion, for easy and practical use in standard training environments. The frontal and lateral acquisition modalities offer distinct advantages and limitations.

The frontal view allows for a more direct measurement of the projected area, and corresponds closely to the true frontal section. However, this approach is sensitive to water transparency and swimmer-to-camera distance, which affect image clarity and segmentation quality. Additionally, the varying scale factor due

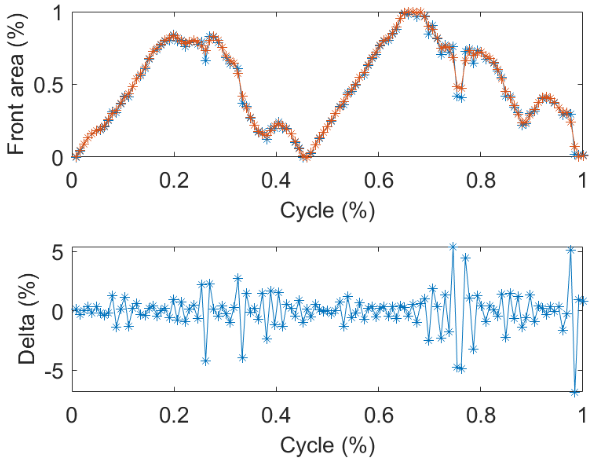


Figure 12. Top: normalized frontal area profile over one stroke cycle: original data in blue; filtered data in red. Bottom: percentage residuals between measured data and the fitted curve.

to perspective introduces challenges in ensuring consistent area estimation across trials.

The lateral view benefits from a shorter operational distance and more stable optical conditions. Although it provides only an indirect 2D representation of the frontal area, it enhances the visibility of body posture and attitude-related features, such as the angle of incidence relative to the water flow. This makes it particularly valuable to assess technique adjustments or streamlining effectiveness.

In both configurations, the system demonstrates sufficient repeatability for comparative analyses, particularly when normalized over the stroke cycle. Although absolute accuracy is limited by the simplified setup, the method remains suitable for tracking intra-athlete changes or evaluating technical interventions by swimming coaches.

## ACKNOWLEDGEMENTS

This work benefited greatly from the expertise and assistance of Dr. Mauro Antonini, Technical Director of the Italian National Deaf Swimming Team: his guidance on the topics of swimming sports training was precious and inspiring.

## REFERENCES

[1] M. Cortesi, R. Di Michele, S. Fantozzi, S. Bartolomei, G. Gatta, Arm-stroke descriptor variability during 200-m front crawl swimming, Sensors, vol. 21, 2021, no. 2, p. 324.
DOI: 10.3390/s21020324

[2] F. Crenna, G. B. Rossi, M. Khalil, Biomechanical movement analysis by inertial sensors: An application to swimming, Measurement: Sensors, vol. 38, 2025, p. 101707.
DOI: 10.1016/j.measen.2024.101707

[3] M. Cortesi, G. Gatta, G. Michielon, R. Di Michele, S. Bartolomei, R. Scurati, Passive drag in young swimmers: Effects of body composition, morphology and gliding position, International Journal of Environmental Research and Public Health, vol. 17, Mar. 2020, no. 6, p. 2002.
DOI: 10.3390/ijerph17062002

[4] M. Cortesi, G. Gatta, R. Carmigniani, P. Zamparo, Estimating active drag based on full and semi-tethered swimming tests, Journal of Sports Science and Medicine, vol. 23, 2024, pp. 17–24.
DOI: 10.52082/jssm.2024.17

[5] G. Gatta, M. Cortesi, I. Swaine, P. Zamparo, Mechanical power, thrust power and propelling efficiency: relationships with elite sprint swimming performance, Journal of Sports Sciences, vol. 36, May 2017, no. 5, pp. 506–512.
DOI: 10.1080/02640414.2017.1322214

[6] S. Kolmogorov, O. Duplishcheva, Active drag, useful mechanical power output and hydrodynamic force coefficient in different swimming strokes at maximal velocity, Journal of Biomechanics, vol. 25, Mar. 1992, no. 3, pp. 311–318.
DOI: 10.1016/0021-9290(92)90028-y

[7] H. M. Toussaint, P. E. Roos, S. Kolmogorov, The determination of drag in front crawl swimming, Journal of Biomechanics, vol. 37, Nov. 2004, no. 11, pp. 1655–1663.
DOI: 10.1016/j.jbiomech.2004.02.020

[8] R. Naemi, S. G. Psycharakis, C. McCabe, C. Connaboy, R. H. Sanders, Relationships between glide efficiency and swimmers' size and shape characteristics, Journal of Applied Biomechanics, vol. 28, Aug. 2012, no. 4, pp. 400–411.
DOI: 10.1123/jab.28.4.400

[9] G. Gatta, M. Cortesi, S. Fantozzi, P. Zamparo, Planimetric frontal area in the four swimming strokes: Implications for drag, energetics and speed, Human Movement Science, vol. 39, Feb. 2015, pp. 41–54.
DOI: 10.1016/j.humov.2014.06.010

[10] E. Ceseracciu, Z. Sawacha, S. Fantozzi, M. Cortesi, G. Gatta, S. Corazza, C. Cobelli, Markerless analysis of front crawl swimming, Journal of Biomechanics, vol. 44, Aug. 2011, no. 12, pp. 2236–2242.
DOI: 10.1016/j.jbiomech.2011.06.003

[11] N. Giulietti, A. Caputo, P. Chiariotti, P. Castellini, SwimmerNET: Underwater 2d swimmer pose estimation exploiting fully convolutional neural networks, Sensors, vol. 23, 2023, no. 9, p. 2364.
DOI: 10.3390/s23042364

[12] Z. Cao, T. Simon, S.-E. Wei, Y. Yang, Openpose: Realtime multi-person 2d pose estimation using part affinity fields, IEEE Transactions on Pattern Analysis and Machine Intelligence, vol. 43, 2021, no. 4, pp. 172–186.
DOI: 10.1109/TPAMI.2019.2929257

[13] J. Redmon, S. Divvala, R. B. Girshick, A. Farhadi, You only look once: Unified, real-time object detection, Proceedings of the IEEE Conference on Computer Vision and Pattern Recognition (CVPR), 2016, pp. 779–788.
DOI: 10.1109/CVPR.2016.91

[14] A. Edriss et al., Commercial vision sensors and ai-based pose estimation frameworks for markerless motion analysis in sports and exercises: a mini review, Frontiers in Physiology, 2025.
DOI: 10.3389/fphys.2025.1649330

[15] S. Patil et al., Ai for swimming recommendation systems exploring the current landscape and research opportunities, Discover Applied Sciences, 2025.
DOI: 10.1007/s42452-025-08156-x

[16] J. M. González-Ravé et al., Towards the determination of the instant active drag using a vision-based system, Sensors, vol. 22, 2022, no. 3, p. 1139.
DOI: https://doi.org/10.3390/s22030955

[17] D.-P. Born, E. Rüeger, C. M. Beaven, M. Romann, Comparing cross-sectional and longitudinal tracking to establish percentile data and assess performance progression in swimmers, Scientific Reports, vol. 12, 2022, no. 1.
DOI: 10.1038/s41598-022-13837-3

[18] S. Washino, A. Murai, T. Kadi, K. Narita, H. Mankyu, Y. Yoshitake, Interpreting the projected frontal area in front crawl: determining the projected frontal area of each body segment, Medicine & Science in Sports & Exercise, vol. 57, 2025, no. 2, pp. 390–399.
DOI: 10.1249/mss.0000000000003564

[19] S. Washino, A. Murai, T. Kadi, H. Mankyu, Y. Yoshitake, Stroke phase differences in the linear relationship between swimming velocity and vertical body position during front crawl, Sports Biomechanics, vol. 24, 2025, pp. 2219–2232.
DOI: 10.1080/14763141.2024.2446180

[20] J. E. Morais, R. H. Sanders, C. Papic, T. M. Barbosa, D. A. Marinho, The influence of the frontal surface area and swim velocity variation in front crawl active drag, Medicine & Science in Sports & Exercise, vol. 52, 2020, no. 11, pp. 2357–2364.
DOI: 10.1249/mss.0000000000002400

[21] R. Vennell, D. Pease, B. Wilson, Wave drag on human swimmers, Journal of Biomechanics, vol. 39, 2006, no. 4, pp. 664–671. DOI: 10.1016/j.jbiomech.2005.01.023
[22] H. M. Toussaint, M. Truijens, Biomechanical aspects of peak performance in human swimming, Animal Biology, vol. 55, 2005, no. 1, pp. 17–40. DOI: 10.1163/1570756053276907
[23] T. M. Barbosa, M. J. Costa, J. E. Morais, Estimating the hydrodynamic profile of swimmers: drag, propulsion and efficiency, Sports Medicine, vol. 51, 2021, no. 9, pp. 1839–1853. DOI: 10.1007/s40279-021-01468-1